Table 3. Percentage abundance of different elements (nuclei with energy 11.4 – 23 MeV per nucleon) relative to oxygen for four time intervals during the flare of November 4 – 7, 2001.

Time	C	N	O	Ne	Mg	Si
22 h 04 Nov – 15 h 05 Nov	39.0 ± 3.9	11.9 ± 1.7	100	14.4 ± 2.3	17.9 ± 2.4	17.4 ± 2.2
22 h 05 Nov – 07 h 06 Nov	45.5 ± 3.4	10.4 ± 1.3	100	12.0 ± 1.4	20.6 ± 2.0	16.8 ± 1.9
07 h 06 Nov – 19 h 06 Nov	42.4 ± 6.5	11.2 ± 2.7	100	12.4 ± 2.7	16.8 ± 3.4	10.4 ± 2.6
19 h 06 Nov – 20 h 07 Nov	54.7 ± 12.6	8.5 ± 2.0	100	12.2 ± 4.6	21.6 ± 6.7	18.9 ± 6.0

indicated an increase in these particle fluxes from the moment of the flare to the CME arrival at the Earth. The shock wave effectively accelerated electrons. The middle panel of Fig. 15 displays the time dependences of the electron fluxes with energy from 0.3 to 12 MeV, which have not been measured by other satellites in this time outside the geomagnetosphere. The upper panel of Fig. 15 shows the electron energy power-law index variations. The electron energy spectrum did not vary significantly as the CME approached the Earth. The electron spectra became softer, and the electron, as well as proton and ion, fluxes started decreasing as the CME receded from the Earth.

The CORONAS-F satellite also measured the ion fluxes with energy from 2 to 40 MeV per nucleon. The time variations of ions from C to Si were similar to proton and electron variations. The chemical composition of ion fluxes over the entire duration of the high-energy particle outburst practically did not change. Table 3 shows the percentage abundance of different elements relative to oxygen for the flare of November 4 – 7, 2001.

Acknowledgments. The authors thank T V Kazachevskaya, Yu D Kotov, G E Kocharov, S N Kuznetsov, N I Lebedev, E P Mazets, A A Nusinov, V M Pankov, A F Podorol'skiĭ, S P Ryumin, and Ya Silwester for providing the processed data from the CORONAS-F satellite, which were used in writing the present paper.

References

1. *The SOHO Mission: Scientific and Technical Aspects of the Instruments* (ESA SP, 0379-6566, № 1104, Compiled by T D Guyenne) (Paris: European Space Agency, 1989)
2. Jimenez A et al. *Astron. Astrophys.* **193** 298 (1988)
3. Avetisyan E A et al. "Rentgenovskaya izobrazhayushchaya spektroskopiya Solntsa v oblasti 1.85 – 335 Å v eksperimente SPIRIT (SRT-K, RES-K) na sputnike KORONAS-F" (X-ray imaging spectroscopy of the Sun at 1.85 – 335 Å in the SPIRIT (SRT-K, RES-K) experiment onboard the CORONAS-F satellite) *Pis'ma Astron. Zh.* (in press)

PACS numbers: 04.40.Dy, **97.60. – s**

DOI: 10.1070/PU2002v045n08ABEH001193

Wolf – Rayet stars and relativistic objects

A M Cherepashchuk

1. Introduction

Wolf – Rayet (WR) stars, identified by strong broad emission lines of helium, nitrogen, carbon, and oxygen at different ionization states, were discovered by French astronomers M Wolf and G Rayet in 1867 [1]. We shall consider only massive ($m = 5 - 50 M_\odot$) WR stars of the galactic type I population, which concentrate on average towards the galactic plane. Low-mass hot stars observed as nuclei of planetary nebulae also exhibit WR signatures; we shall not consider them in the present paper.

In total, 227 WR stars are known in our Galaxy and about 300 in nearby galaxies [2]. The full number of WR stars in the Galaxy is estimated to be one – two thousand.

Recently, a close relation between WR star evolution and the formation of neutron stars (NS) and black holes (BH) [3 – 5], as well as cosmic gamma-ray burst generation [6, 7], has been revealed.

2. On the nature of WR stars

According to modern concepts, WR stars are the naked helium cores of originally massive ($m > 30 - 40\ M_\odot$) stars that lost most of their hydrogen envelopes either as a result of mass exchange in close binary systems (CBS) [8], or due to intensive mass outflow from single stars in the form of stellar wind [9, 10]. The powerful emission line spectrum of WR stars forms at the base of stellar wind moving with velocities of 1 – 3 thousand km s^{-1} apparently due to radiation pressure from the hot 'core' at a rate of $\sim 10^{-5}\ M_\odot$ per year (see monographs [11, 12] and references therein). The mechanism of the WR wind acceleration has not yet been finally established.

WR stars are subdivided into two sequences: the nitrogen one (WN) and the carbon one (WC). The spectra of WN stars are mainly dominated by nitrogen lines, while WC spectra mostly show the presence of carbon and oxygen. Besides, among WR stars a small group of stars with enhanced oxygen lines (WO-stars) can be separated.

The spectra of WN and WC stars show both helium and hydrogen lines, however the hydrogen lines are very weak due to the predominantly helium chemical composition of WR stars. The sequence WN – WC – WO is interpreted as an evolutionary one [8]. Immediately after the massive star core exposure, it is enriched by products of the CNO-cycle of thermonuclear reactions. So initially the surface of the WR-star is enriched with nitrogen (the WN-stage). As the star loses mass via stellar wind, the layers enriched with carbon due to thermonuclear conversion of helium in triple α-particle collisions are exposed (the WC-stage). The subsequent mass loss exposes the WR star layers enriched with oxygen due to the reaction of α-particle captures by carbon atoms (the WO-stage). The mean mass of the WN stars is $\sim 22\ M_\odot$ and of the WC stars is $12\ M_\odot$, which is qualitatively consistent with the described evolutionary scenario for WR stars. About half of WR stars occur in binary systems WR + O which contain massive hot stars of spectral class O as companions.

WR stars, as massive, hot, non-degenerate, mainly helium stars at late evolutionary stages, must explode as type Ib or type Ic supernovae and form relativistic objects as a result of the collapse of their CO-cores. Besides, the absence of

powerful hydrogen envelopes in WR stars facilitates the collapse energy transformation into the observed gamma-ray emission in some cases [6, 7]. To date, the masses of 23 WR stars in binary WR + O systems and of 34 relativistic objects (19 NS and 15 BH) in X-ray binary systems and binary systems with radio pulsars have been measured (see reviews [4, 13–16] and references therein, as well as recent publications [17–20]).

It appears interesting to match the masses of WR stars and their CO-cores at the end of their evolution with the masses of relativistic objects. Both WR stars and other massive stars, for example, red and blue supergiants with normal chemical surface composition can be progenitors of relativistic objects. However, as we are studying the masses of relativistic objects and WR stars in binary systems only, the comparison of the NS and BH masses with the WR star masses is correct, since a massive star rapidly loses its hydrogen envelope in a binary system and transforms into a WR star [8]. In most evolutionary scenarios for CBS containing a massive star, the latter ultimately forms a WR star whose core collapses into a NS or BH (see, for example, [21, 22]). Only in the case of radio pulsars in binary systems with circular orbits and low-mass white dwarf companions has the possibility of the NS formation from the collapse of a white dwarf with mass increased up to the Chandrasekhar limit by accretion of matter from a low-mass non-degenerate companion been discussed [21]. Thus, we can consider all NS and BH in X-ray binary systems and most NSs-radio pulsars in binary systems to originate from the collapse of CO-cores of WR stars.

3. The distribution of masses of relativistic objects

Papers [3, 23] noted that the observed mass distribution of the relativistic objects in CBS is bimodal: the NS masses lie within the narrow range $m_{\rm NS} = (1-2)\,M_\odot$, the BH masses are concentrated inside the interval $m_{\rm BH} = (4-16)\,M_\odot$. The most recent data on relativistic object mass determinations are listed in Table 1 and shown in Fig. 1. It is seen that there is no relation between relativistic object masses and their companion masses in CBS. We also stress that the measured masses of X-ray and radio pulsars (NS) do not exceed $3M_\odot$, the theoretical upper NS mass limit predicted by A. Einstein's theory of general relativity (GR). Besides, none of the 15 massive ($m_{\rm x} > 3\,M_\odot$) compact X-ray sources in CBS (BH candidates) is either an X-ray pulsar or a type I X-ray burster, also in accordance with the GR predictions.

Table 1. Parameters of binary systems with black holes.

System	Optical star spectrum	$P_{\rm orb}$, days	$f_{\rm v}(m)$, $M_\odot$	$m_{\rm x}$, $M_\odot$	$m_{\rm v}$, $M_\odot$	$V_{\rm pec}$, km s^{-1}	Remark
Cyg X-1 V 1357 Cyg	O 9.7 Iab	5.6	0.24 ± 0.01	16 ± 5	33 ± 9	2.4 ± 1.2	persistent
LMC X-3	B3 Ve	1.7	2.3 ± 0.3	9 ± 2	6 ± 2	—	persistent
LMC X-1	O (7–9) III	4.2	0.14 ± 0.05	7 ± 3	22 ± 4	—	persistent
AO 620-00 (V616 Mon)	K5V	0.3	2.91 ± 0.08	10 ± 5	0.6 ± 0.1	-15 ± 5	transient
GS 2023 + 338 (V404 Cyg)	KO IV	6.5	6.08 ± 0.06	12 ± 2	0.7 ± 0.1	8.5 ± 2.2	transient
GRS 1124-68 (GU Mus)	K2 V	0.4	3.01 ± 0.15	$6(+5, -2)$	0.8 ± 0.1	26 ± 5	transient
GS 2000 + 25 (QZ Vul)	K5 V	0.3	4.97 ± 0.10	10 ± 4	0.5 ± 0.1	—	transient
GRO J0422 + 32 (V 518 Per)	M2 V	0.2	1.13 ± 0.09	10 ± 5	0.4 ± 0.1	—	transient
GRO J1655-40 (XNSco1994)	F5 IV	2.6	2.73 ± 0.09	7 ± 1	2.5 ± 0.8	-114 ± 19	transient
H 1705-250 (V2107 Oph)	K5 V	0.5	4.86 ± 0.13	6 ± 1	0.4 ± 0.1	38 ± 20	transient
4U 1543-47 (HL Lup)	A2 V	1.1	0.22 ± 0.02	5 ± 2.5	~ 2.5	—	transient
GRS 1009-45 (MM Vel)	(K6–MO)V	0.3	3.17 ± 0.12	3.6–4.7	0.5–0.7	—	transient
SAX J1819.3-2525 (V4641Sgr)	B9III	2.8	2.74 ± 0.12	$9.61(+2.08, -0.88)$	$6.53(+1.6, -1.03)$	—	transient
XTE 1118 + 480	(K7–MO)V	0.17	6.1 ± 0.3	6.0–7.7	0.09–0.5	—	transient
GRS 1915 + 105	(K–M)III	33.5	9.5 ± 3.0	14 ± 4	1.2 ± 0.2	—	transient

Remark: see reviews [4, 5] and references therein, as well as recent papers [17–19]. Here $P_{\rm orb}$ is the orbital period; $f_{\rm v}(m) = m_{\rm x}^3 \sin^3 i/[(m_{\rm x} + m_{\rm v})^2]$ is the optical star mass function; $m_{\rm x}$, $m_{\rm v}$ are the masses of the relativistic object and the optical star, respectively; and $V_{\rm pec}$ is the peculiar radial velocity of the binary system barycenter.

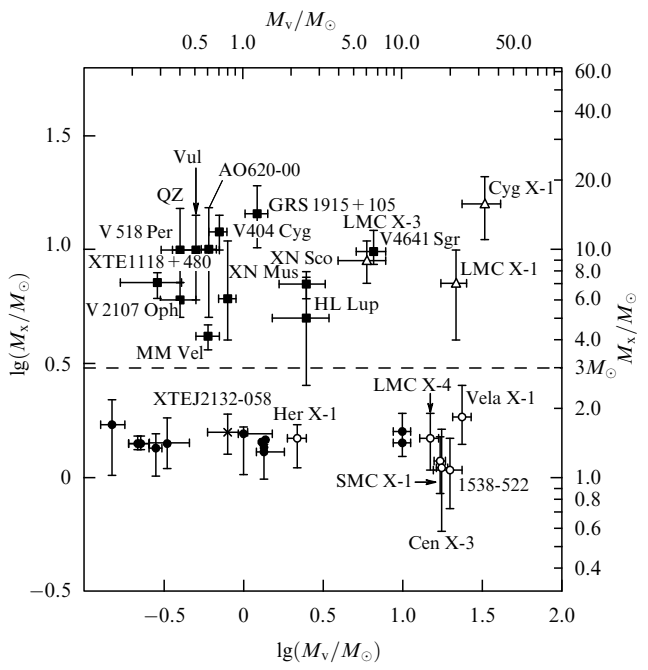

Figure 1. Masses M_x of neutron stars (circles and the cross) and black holes (triangles and squares) as a function of the companion mass M_v in CBS. The filled and open circles correspond to radio and X-ray pulsars, respectively, the cross marks the neutron star in X-ray nova XTE J2132-058 [20]. The filled squares correspond to black holes in X-ray novae, the open triangles stand for black holes in quasi-stationary X-ray binary systems with O-B companions.

The recent data confirm the conclusion on the bimodal distribution of masses of relativistic objects [3, 23]. The masses of 19 NSs lie within narrow limits: $m_{NS} = (1-2)\,M_\odot$, the mean NS mass being $m_{NS} = (1.35 \pm 0.15)\,M_\odot$. The mean mass of NSs-radio pulsars in well-studied CBSs is $(1.35 \pm 0.04)\,M_\odot$ [16]. New spectral observations reported in paper [24] confirm a comparatively high mass value for the NS in X-ray binary system Vela X-1: $m_{NS} = 1.86 \pm 0.16\,M_\odot$, which bears an important meaning to specify the NS equation of state. However, even this highest value of m_{NS} is below $2\,M_\odot$.

The measured masses of 15 BHs in CBS lie within the range $m_{BH} = (4-16)\,M_\odot$ with a mean value of $\bar{m}_{BH} = (8-10)\,M_\odot$. Inside the mass interval $m_x = (2-4)\,M_\odot$ in CBS neither NSs nor BHs have been observed. This gap in the relativistic object mass distribution apparently cannot be explained by observational selection effects [5, 23]. Let us consider such possible effects that could lead to the observed bimodal relativistic object mass distribution in CBS, though the actual NS and BH mass distributions can be continuous.

1. The disruption of a CBS in the relativistic object mass interval $(2-4)\,M_\odot$ caused by the supernova explosion and the loss of more than half the total mass of the CBS [5]. Such a CBS disruption is most probable for systems containing the least massive relativistic objects, i.e. NSs, which contradicts observations: there are many low-mass X-ray binaries with NSs, and the fraction of binaries with NSs among X-ray novae is $\sim 30\,\%$ [4].

2. The heating and stabilization of the accretion disc in CBS by X-ray radiation from the central accreting relativistic object. It is argued [15] that this effect in the relativistic object mass range $(2-4)\,M_\odot$ makes all X-ray novae occur in a permanent high state, which precludes the lines of the companion from being seen in the spectrum and the relativistic mass object from being measured. But the conditions for the accretion disk illumination are most favorable for accreting NSs. At the same time, about 30% of X-ray novae contain NSs.

3. A strong stellar wind mass loss by WR stars in binary systems, which can lead to the formation of only NSs in CBS and low-mass BHs do not form [25]. As was noted in Refs [3, 4], accounting for a clumpy structure of WR stellar winds several times decreases the WR mass loss rate, so the radial mass loss by the WR star should not strongly prevent low-mass BH formation.

4. Accretion of matter in binary systems increases the mass of NSs and BHs, so their masses can be systematically different from masses of single NSs and BHs. Paper [4] shows this effect to be also insignificant, the mass difference between single NSs and BHs and entering CBS must be negligible because, in particular, most companions in CBS-X-ray novae are low-mass K – M main-sequence dwarfs which cannot provide a significant mass increase of accreting relativistic objects.

Thus, it is hard to invent an observational selection effect which would depend on the relativistic mass object in such a non-monotonic way and provide the observed gap in the mass distribution of NSs and BHs at $(2-4)\,M_\odot$. There are all grounds to consider this gap as real: for some reason, very massive NSs ($m_{NS} > 2\,M_\odot$) and low-mass BHs ($m_{BH} < 4\,M_\odot$) do not form in binary systems. Considering the above argumentation, this conclusion may be also related to single relativistic objects.

4. Distribution of masses of WR stars and their CO-cores in the end of evolution

In matching the masses of relativistic objects and WR stars, the radial stellar wind mass loss at a rate of $\dot{M}_{WR} \cong 10^{-5} M_\odot$ per year should be taken into account. For the first time, the mass loss of WR stars depending on the mass of the star M_{WR} was considered in Ref. [26]:

$$\dot{M}_{WR} = -(0.6-1.0) \times 10^{-7} \left(\frac{M_{WR}}{M_\odot}\right)^{2.5}. \qquad (1)$$

The use of this formula leads to the well-known convergence effect: almost irrespective of the initial mass of a WR star, the mass of its CO-core at the end of evolution, M_{CO}^{f}, is very small, $M_{CO}^{f} \approx 3\,M_\odot$. But then how can one understand the existence of BHs with masses $(10-15)\,M_\odot$ (see Table 1 and Fig. 1)?

The final masses of WR stars and their CO-cores, with account for the clumpy structure of the WR winds, which decreases the values of $\dot{M}_{WR}$ approximately by a factor of three, were calculated in paper [5]. In that paper, the empirical relation

$$\dot{M}_{WR} = k M_{WR}^{\alpha}, \qquad (2)$$

was employed that was obtained from analysis of polarization observations of around ten binary WR + O systems [27]. According to [27], in Eqn (2) $\alpha = 1-2$, with $\alpha = 1$ being the preferential value.

The clumpy structure of the WR winds was revealed in papers [28, 29]. The clumpy structure of a stellar wind accelerated by the radiation pressure in lines can be the

manifestation of some instabilities due to, in particular, the dependence of the effective radiation acceleration of the stellar wind matter on velocity gradients inside it [12]. As noted in Ref. [30], since the intensity of thermal radio and IR emission depends quadratically on density, the values of $\dot{M}_{\rm WR}$ for WR stars inferred from the analysis of their radio and IR fluxes in the model of the continuous wind have been overestimated by several times. Accounting for the clumpy structure of WR star winds decreases the coefficient k 2–4 times [see Eqn (2)]; this and also the lower power-law index $\alpha = 1-2$ in Eqn (2) allow the above mentioned convergence effect to be avoided. The results of calculations of the final masses of CO-cores of WR stars with known masses [5] are summarized in Fig. 2 which shows the mass distribution for 34 relativistic objects and final CO-cores $M_{\rm CO}^{\rm f}$ of 23 WR stars with known masses (for the cases $\alpha=1$ and $\alpha=2$). Apparently, the mass distribution $M_{\rm CO}^{\rm f}$ is broad, $M_{\rm CO}^{\rm f}=(1-2)M_\odot-(20-44)\,M_\odot$, and continuous in the mass interval of interest $(1-12)\,M_\odot$. The dips in the distribution $M_{\rm CO}^{\rm f}$ at $M_{\rm CO}^{\rm f} > 12\,M_\odot$ are due to the small number of observed WR stars with large masses. Thus, the masses of CO-cores of WR stars at the end of evolution, $M_{\rm CO}^{\rm f} = (1-2)\,M_\odot-(20-44)\,M_\odot$, comprise the observed mass range of the relativistic objects $m_{\rm x} = (1-16)\,M_\odot$. The mean mass $\bar{M}_{\rm CO}^{\rm f} = 7.7\,M_\odot$ for $\alpha = 2$ and $\bar{M}_{\rm CO}^{\rm f} = 10.6\,M_\odot$ for $\alpha = 1$. The mean CO-core mass, $\bar{M}_{\rm CO}^{\rm f} = (7.7-10.6)\,M_\odot$, is close to the mean BH mass $\bar{M}_{\rm BH} = (8-10)\,M_\odot$.

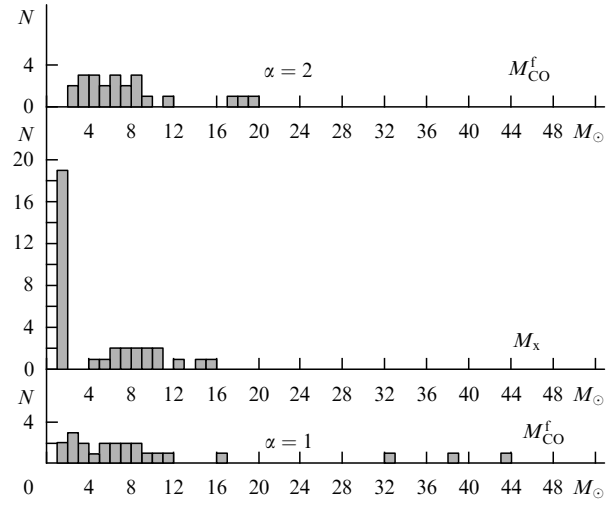

Figure 2. Histograms of the final mass distribution of the carbon-oxygen cores $M_{\rm CO}^{\rm f}$ for 23 WR stars with known masses (the bottom and upper panels correspond to the case $\alpha + 1$ and $\alpha = 2$ in Eqn (2), respectively). The middle panel shows the distribution of masses $M_{\rm x}$ of 34 relativistic objects in CBS. The high peak in the $(1-2)\,M_\odot$ range corresponds to NSs. The $M_{\rm CO}^{\rm f}$ distributions are continuous, while the $M_{\rm x}$ distribution is bimodal with a gap in the mass range $M_{\rm x} = (2-4)\,M_\odot$.

5. Conclusions

The observed mass distribution of the relativistic objects is bimodal ($m_{\rm NS} = (1-2)\,M_\odot$, $m_{\rm BH} = (4-16)\,M_\odot$), in spite of the mass distribution of their progenitors, the CO-cores of WR stars at the end of evolution, being continuous [$M_{\rm CO}^{\rm f} = (1-2)\,M_\odot-(20-44)\,M_\odot$]. Such a difference in the mass distributions provides grounds to assume that not only the progenitor's mass determines the nature of the relativistic object formed (neutron star, black hole), but other parameters of the progenitor, such as magnetic field, rotation, the statistical outcome of the collapse due to different instabilities, etc. (see, for example, Ref. [31]) are also important. Recently rotational effects have been discovered in some WR stars by depolarization of radiation in emission lines (see, for example, Ref. [32]). The fraction of rapidly rotating WR stars is 15–20% [32].

Further studies of differences in the mass distribution of the relativistic objects and their progenitors — CO-cores of WR stars seem to be very promising. Intensive observations of both relativistic objects and WR stars in CBS are required.

Paper [33] suggests a qualitative explanation of the dip in the observed NS and BH mass distribution by assuming a fairly soft equation of state of NS matter (the upper limit of the NS mass $\sim 1.5\,M_\odot$) and considering the magnetorotational mechanism of supernova explosion [34], which under certain conditions prevents the fall-back of a fraction of the ejected envelope onto the newly formed, rapidly rotating, and strongly magnetized NS resulting from the collapse. Paper [7] argues that core collapses of WR stars deprived of their hydrogen envelopes can give rise to cosmic gamma-ray bursts; in particular, the large dispersion of the final CO-core masses of WR stars and the bimodal mass distribution of the relativistic objects match the large spread of the observed gamma-ray burst energies and their possible bimodal distribution.

Recently, some evidence has been found for the possible bimodal distribution of the luminosity at the maximum brightness of 18 well-studied type Ibc supernovae [35]. The mean absolute stellar magnitude in blue light at the maximum brightness is $M_{\rm B} = -17^m.61$ for normal type Ibc supernovae (13 objects) and $M_{\rm B} = -20^m.26$ for bright supernovae of this type (5 objects). So the maximum luminosities of normal and bright type Ibc supernovae differ by an order of magnitude. If this result is confirmed in further observations, there will be grounds to argue that not only the final collapse products of the CO-cores of WR stars have a bimodal mass distribution but also the concomitant supernovae have a bimodal explosion energy distribution.

Theoretical investigations in these directions (see, for example, [33, 34, 36, 37]) appear very promising.

References

1. Wolf M, Rayet G *C.R. Acad. Sci.* **65** 292 (1867)
2. Van der Hucht K A *New Astron. Rev.* **45** 135 (2001)
3. Cherepashchuk A M, in *Modern Problems of Stellar Evolution: Proc. of the Intern. Conf. in Honour of Professor A G Massevitch's 80th Birthday, Zvenigorod, Russia, 13–15 October 1998* (Ed. D S Wiebe) (Moscow: GEOS, 1998) p. 198
4. Cherepashchuk A M *Space Sci. Rev.* **93** 473 (2000)
5. Cherepashchuk A M *Astron. Zh.* **78** 145 (2001) [*Astron. Rep.* **45** 120 (2001)]
6. Gershteĭn S S *Pis'ma Astron. Zh.* **26** 848 (2000) [*Astron. Lett.* **26** 730 (2000)]
7. Postnov K A, Cherepashchuk A M *Astron. Zh.* **78** 602 (2001) [*Astron. Rep.* **45** 517 (2001)]
8. Paczynski B, in *Wolf–Rayet and High-Temperature Stars: Symp. No. 49 of the Intern. Astron. Union, Buenos Aires, Argentina, Aug. 9–14, 1971* (Eds M K V Bappu, J Sahade) (Dordrecht: D. Reidel Publ. Co., 1973) p. 143
9. Conti P S *Mem. Soc. R. Sci. Liege* **9** (6) 193 (1976)
10. Bisnovatyi-Kogan G S, Nadyozhin D K *Astrophys. Space Sci.* **15** 353 (1972)
11. De Jager C *The Brightest Stars* (Dordrecht: D. Reidel Publ. Co., 1980) [Translated into Russian (Moscow: Mir, 1984)]

12. Lamers H J G L M, Cassinelli J P *Introduction to Stellar Winds* (Cambridge: Cambridge Univ. Press, 1999) p. 248
13. Novikov I D, Frolov V P *Usp. Fiz. Nauk* **171** 307 (2001) [*Phys. Usp.* **44** 291 (2001)]
14. Cherepashchuk A M *Usp. Fiz. Nauk* **171** 864 (2001) [*Phys. Usp.* **44** 821 (2001)]
15. Charles P, in *Black Holes in Binaries and Galactic Nuclei* (Eds L Kaper, E P J van den Heuvel, P A Woudt) (Berlin: Springer, 2001) p. 27
16. Thorsett S E, Chakrabarty D *Astrophys. J.* **512** 288 (1999)
17. Orosz J A et al., astro-ph/0103045 (submitted to *Astrophys. J.*)
18. Wagner R M et al., Preprint (2001)
19. Greiner J, Cuby J G, McCaughrean M J *Nature* **414** 522 (2001)
20. Casares J et al. *Mon. Not. R. Astron. Soc.* **329** 29 (2002)
21. Shore S N, Livio M, van den Heuvel E P J *Interacting Binaries* (Berlin: Springer-Verlag, 1994)
22. Iben I (Jr), Tutukov A V, Yungelson L R *Astrophys. J. Suppl.* **100** 233 (1995)
23. Bailyn C D et al. *Astrophys. J.* **499** 367 (1998)
24. Barziv O et al. *Astron. Astrophys.* (2002) (in press)
25. Wijers R A M, in *Evolutionary Processes in Binary Stars* (NATO ASI Series, Ser. C, Vol. 477, Eds R A M J Wijers, M B Davies, C A Tout) (Dordrecht: Kluwer Acad., 1996) p. 327
26. Langer N *Astron. Astrophys.* **220** 135 (1989)
27. Moffat A F J, in *Wolf–Rayet Stars: Binaries, Colliding Winds, Evolution: Proc. of the 163rd Symp. of the Intern. Astron. Union, La Biadola, Elba, Italia, May 2–6, 1994* (Eds K A van der Hucht, P M Williams) (Dordrecht: Kluwer Acad., 1995) p. 213
28. Cherepashchuk A M, Khaliullin Kh F, Eaton J A *Astrophys. J.* **281** 774 (1984)
29. Moffat A F J et al. *Astrophys. J.* **334** 1038 (1988)
30. Cherepashchuk A M *Astron. Zh.* **67** 955 (1990) [*Sov. Astron.* **34** 481 (1990)]
31. Ergma E, van den Heuvel E P J *Astron. Astrophys.* **331** L29 (1998)
32. Harries T J, Hillier D J, Howarth I D *Mon. Not. R. Astron. Soc.* **296** 1072 (1998)
33. Postnov K A, Prokhorov M E *Astron. Zh.* **78** 1025 (2001) [*Astron. Rep.* **45** 899 (2001)]
34. Bisnovatyĭ-Kogan G S *Astron. Zh.* **47** 813 (1970) [*Sov. Astron.* **14** 652 (1971)]
35. Richardson D et al. *Astrophys. J.* **123** 745 (2002); astro-ph/0112051
36. Ivanova L N, Chechetkin V M *Astron. Zh.* **58** 1028 (1981) [*Sov. Astron.* **25** 584 (1981)]
37. Ensman L M, Woosley S E *Astrophys. J.* **333** 754 (1988)

PACS number: 97.60.Bw

DOI: 10.1070/PU2002v045n08ABEH001192

Type Ib/c supernovae: new observational data

D Yu Tsvetkov

1. Introduction

The evolution of stars of certain classes ends up with a supernova explosion after which the star disappears or transforms into a qualitatively different state. Supernova explosions (SN) are observed in galaxies as a sudden appearance of a star with luminosity comparable with the total luminosity of the host galaxy.

In recent years, the interest in supernova studies has grown strongly. Twenty years ago less than 20 supernovae were discovered per year, ten years ago this number increased to 60, and in 2001 a record number of supernovae (282) were discovered. The total number of extragalactic supernovae discovered since 1885 is already more than 2000. To search for supernovae, special fully automatic systems have been elaborated. Amateur astronomers also actively participate in SN searches.

Observational astrophysics studies the dependence of the SN emission power on time — the light curves in various spectral bands, and their spectral changes with time.

Statistical studies of the SN population, such as the explosion rate determination, the spatial distribution inside the host galaxies, etc., are also carried out.

Theoretical light curve and spectra modeling, as well as the statistical characteristics, allow astronomers to conclude which stars explode as supernovae and what may be supernova remnants.

2. Classification of supernovae

Even at the very beginning of supernova studies it became clear that they do not represent a homogeneous class of objects. The existing classification is mainly based on the spectral shape near the maximum brightness. Supernovae were subdivided in two main types, I and II. The spectra of the type II supernovae demonstrated bright emission hydrogen lines, while SN I did not. SN I occur in all types of galaxies, including ellipticals, where the star formation has almost stopped by now, while SN II reside only in spiral galaxies and clearly demonstrate concentration towards spiral arms. The principal features in the type I supernova spectra near the maximum brightness were broad absorption lines of single-ionized elements of intermediate mass, such as silicon, calcium, magnesium, sodium, and iron. One of the most prominent features was the absorption line of Si II at the wavelength 6150 Å. As early as in the 1960s, it was noted that in the spectra of some SN I this line is weak or almost absent. Those supernovae were termed peculiar type I supernovae. Only in the middle of the 1980s did it become clear that these supernovae constitute a special class notably different from SN I. The spectra of these supernovae were obtained with digital detectors which allowed exact measurements of the line intensities. But most significant were studies of spectra obtained at the late (> 200 days after the maximum) stage after the explosion. These spectra proved totally different from most SN I. They were dominated by forbidden emission lines of oxygen and calcium, while in spectra of usual SN I at these phases blends of the iron and cobalt lines are most prominent. It was also established that these 'peculiar' SN I occur only in spiral galaxies and demonstrate a close relation to star forming regions inside them. Therefore, these supernovae were shown to be not a variety of SN I, but constitute a special supernova type, whose presupernova evolutionary status is rather like SN II. This type was named Ib, and 'ordinary' type I supernovae were designated as Ia. A more detailed investigation of the SN Ib spectra revealed that the most prominent absorption lines in their spectra near the maximum brightness at wavelengths around 5700 Å belong to helium. Lines of calcium, silicon, and iron, typical for SN Ia, were also present. As the number of studied SN Ib grew, differences in their spectra became apparent. The most clear difference was in the helium line intensities; in some SN Ib they were almost absent. Those supernovae were proposed to be called type Ic. However, at the late nebular stage, they showed no spectral differences with SN Ib. It was also shown that in the SN Ic spectra helium is present, so most likely there are not separate type Ib and Ic SNs, but a continuous sequence of spectral characteristics related to different helium abundance in the envelope.